Water renewal timescales in an ecological reconstructed lagoon in China

Xueping Gao, Yuanyuan Chen and Chen Zhang

ABSTRACT

To improve water quality and construct a landscape lagoon in China, an ecological reconstruction plan for the Qilihai Lagoon (Changli County, Hebei) is proposed. A three-dimensional numerical model (EFDC) was used to study the water renewal capacity in the reconstructed lagoon by using residence time, exposure time and connectivity as timescales. The influences of wind and the depth of the tidal inlet of the lagoon on water renewal capacity were also investigated. The results show that the transport and diffusion processes in the lagoon were strongly influenced by wind and the modification of the tidal inlet. The lagoon under a no wind condition exhibited a low water renewal capacity, especially at the end areas (exposure time, 700–1,000 days). The wind action notably enhanced the water renewal capacity in the lagoon, and the exposure times were all lower than 400 days in the whole region. The optimal inlet depth for the water renewal in the lagoon was predicted to be 4.0 m. The connectivity matrices identified which areas of the domain would be most affected by a pollution source under different conditions. This study examines transport and diffusion processes in a reconstructed lagoon, which could be informative for ecological reconstruction planning.

Key words | connectivity matrix, ecological reconstruction, exposure time, Qilihai Lagoon, residence time, water renewal

Xueping Gao (corresponding author)
Yuanyuan Chen
Chen Zhang
State Key Laboratory of Hydraulic Engineering
Simulation and Safety,
Tianjin University,
Tianjin 300072,
China
E-mail: *xpgao@tju.edu.cn*

INTRODUCTION

The health of a lagoon ecosystem is governed by its physical, chemical, and biological processes. One physical process that affects the health and water quality of the system and indicates its susceptibility to impairment is the water renewal capacity between the lagoon and the open sea (Arega *et al.* 2008). Through the advection and diffusion mechanisms, the water mass is transported to the open sea where it is mixed with the seawater. During this process, pollutants are neutralised and mechanically removed from the ecological compartment. Various time scales are useful tools to estimate the water renewal capacity between the lagoon and the open sea, such as renewal time (Ribbe *et al.* 2008), age (Monsen *et al.* 2002; Li *et al.* 2011; Shen *et al.* 2011; Brye *et al.* 2012), residence time (Arega *et al.* 2008; Cucco & Umgiesser 2006; Delhez & Deleersnijder 2006) and exposure time (Delhez 2006; Brauwere *et al.* 2011).

In this study, we focus on two timescales to estimate the water renewal process: residence time and exposure time. Both timescales measure the time spent by a water parcel or a pollutant in a given water body. The residence time is usually defined as the time taken for a water parcel to leave the region of interest for the first time, which means the water parcel must vanish at the boundary of the region of the interest. The exposure time is defined as the accumulated time spent by a water parcel in the region of interest before the water parcel leaves the region definitively. In a tidal system, when the tide rises in a lagoon, new water is mixed with the existing water; when the tide falls, the water is discharged out of the lagoon. Some part of the discharged water is lost and mixed with the sea, while the remainder returns to the lagoon in the subsequent flow. In this situation not all the water entering in the incoming

tide is 'new water' determining a difference between residence time and exposure time (Cucco & Umgiesser 2006).

We aim to study the transport and diffusion process in a reconstructed lagoon (Qilihai Lagoon) in China using residence time, exposure time using a three-dimensional numerical model. The impact of meteorological factors (such as wind forcing) on the water bodies was also investigated. This work also examines the potential impact of anthropic modifications to the tidal inlet on water bodies. Specifically the water renewal capacity and the transport and diffusion processes of dissolved pollutants under different tidal inlet depths are analysed. Detailed tasks of this study are as follows: (1) to divide the lagoon into nine subregions and compute the residence and exposure times for each subregion to estimate the water renewal capacity in the reconstructed lagoon when only tide forces the circulation; (2) to decompose the exposure time into subregion exposure time, resulting in a connectivity matrix, and to estimate the transport and diffusion of pollutants in the reconstructed lagoon when only the tide forces the circulation; (3) to compute the exposure time and connectivity when the wind is prescribed and forces the circulation together with tide and to estimate the influence of wind on water renewal in the reconstructed Qilihai Lagoon; and (4) to compute the exposure time and connectivity under different depths of the inlet when the tide forces the circulation and to estimate the influence of inlet depth on water renewal in the reconstructed Qilihai Lagoon.

METHODS

Study area

The Qilihai Lagoon (Figure 1) is a shallow lagoon situated in Changli County, Hebei Province (39°34′ 41.50″ N, 119°17′ 9.49″ E). The lagoon is connected to the Liaodong Bay by a narrow inlet, through which water is exchanged between the lagoon and the sea. The Qilihai Lagoon has been severely polluted since the 1970s due to extensive human activities, including recreation, fish farming and socialising by visitors and local residents. To improve the water quality and to build a landscape lagoon, the local authorities decided to restore and reconstruct the lagoon. The lagoon in the present configuration has a total surface area of approximately 3.50 million m^2 and is very shallow, with an average depth of 1.0 m (Figure 1(a)). Several measures have been introduced for ecological reconstruction planning. The first measure concerns expanding the water area of the lagoon. The shrimp ponds and beaches to the southwest of the lagoon will be reconstructed so that they will become part of the lagoon, increasing the new lagoon's total surface area to 9.65 million m^2. The second measure concerns dredging the lagoon and cleaning the mud in the lagoon. After reconstruction, the average depth in the central part of the lagoon will increase to 2.5 m and the depth in the inlet will be 3.5 m. Finally, two artificial islands will
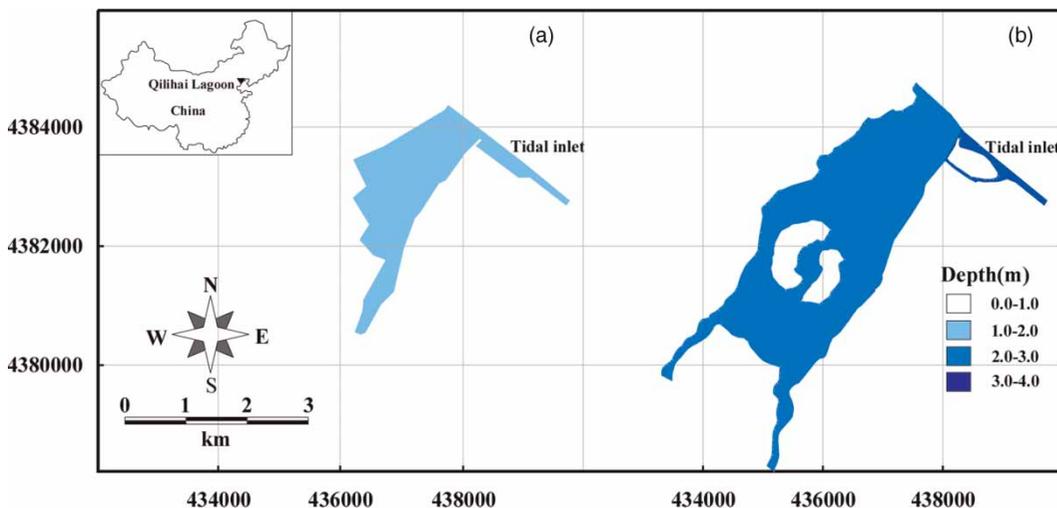

Figure 1 | Location and map of Qiqihai Lagoon: (a) The lagoon in the present configuration. (b) The lagoon in the ecologically reconstructed configuration.

be built for the purposes of landscape and recreation. Ecological parks, entertainment and culture centres, and resort hotels will be built on the island. The Qilihai Lagoon will be reconstructed into an ecological landscape lagoon as an entertainment and culture centre. The prevised shape of the ecologically reconstructed lagoon is shown in Figure 1(b).

Numerical model

The three-dimensional Environmental Fluid Dynamics Code (EFDC) model was used for the simulations in this study. Details of the EFDC model are documented by Hamrick (1992). The model has been extensively applied and documented for modelling circulation, thermal stratification, sediment transport, water quality, and eutrophication in numerous lakes, rivers, and estuaries (Ji *et al.* 2002; Jin & Ji 2004; Sebnem 2008; Zhang *et al.* in press).

In the EFDC model, the hydrodynamics equations may be expressed in terms of Equation (1) to Equation (4), which are two momentum equations (Equation (1) and Equation (2)), a vertical hydrostatic pressure relationship equation (Equation (3)), and a continuity equation (Equation (4)). The governing mass-balance equation for the passive tracer may be expressed as Equation (5):

$$
\begin{aligned}
&\partial_t(mHu) + \partial_x(m_y Huu) + \partial_y(m_x Hvu) + \partial_z(mwu) \\
&\quad - (mf + v\partial_x m_y - u\partial_y m_x)Hv \\
&= -m_y H\partial_x(g\xi + p) - m_y(\partial_x h - z\partial_x H)\partial_z p \\
&\quad + \partial_z((mH^{-1})A_v\partial_z u) + Q_u
\end{aligned}
\tag{1}
$$

$$
\begin{aligned}
&\partial_t(mHv) + \partial_x(m_y Huv) + \partial_y(m_x Hvu) + \partial_z(mwu) \\
&\quad + (mf + v\partial_x m_y - u\partial_y m_x)Hu \\
&= -m_x H\partial_y(g\xi + p) - m_x(\partial_y h - z\partial_y H)\partial_z p \\
&\quad + \partial_z(mH^{-1}A_v\partial_z v) + Q_v
\end{aligned}
\tag{2}
$$

$$
\partial_z p = -ghb = -gH(\rho - \rho_0)\rho_0^{-1}
\tag{3}
$$

$$
\partial_t(m\xi) + \partial_x(m_y Hu) + \partial_y(m_x Hv) + \partial_z(mw) = 0
\tag{4}
$$

$$
\begin{aligned}
&\partial_t(mHC) + \partial_x(m_y HuC) + \partial_y(m_x HvC) + \partial_z(mwC) \\
&= \partial_z(mH^{-1}A_b\partial_z C)
\end{aligned}
\tag{5}
$$

where u and v are the horizontal velocity components in the curvilinear, orthogonal coordinates x and y; m_x and m_y are the square roots of the diagonal components of the matrix tensor; and $m = m_x m_y$ is the Jacobian or square root of the metric tensor determinant. The total depth, $H = h + \zeta$, is the sum of the depth below the free surface displacement relative to the undisturbed physical vertical coordinate origin, $z^* = 0$. The pressure p is the relative hydrostatic pressure in the water column, where ρ and ρ_0 are the actual and reference water densities. The density, ρ, is generally a function of temperature, T, and salinity S; and b is the buoyancy, which is defined in the equation as the normalised deviation of density from the reference value (Hamrick 1992). In the momentum equations, f is the Coriolis parameter, A_v is the vertical turbulent or eddy viscosity, A_b is the vertical turbulent diffusivity, and Q_u and Q_v are momentum source–sink terms.

The numerical solution of the EFDC model equations uses a finite volume-finite difference spatial discretisation with a marker-and-cell or C grid staggering of the discrete variables. For simplicity, numerical discretisation is not presented in this paper but is detailed in the EFDC documents (Hamrick 1992).

Water renewal timescales

Residence time

The residence time (R) is usually defined as the time taken for a water parcel to leave the control domain for the first time. There are two different methods for computing the residence time. One is the adjoint approach (Delhez *et al.* 2006), which can be used to compute the residence time for any initial time and any initial location. The adjoint approach is not easy to implement, however. The other is the Lagrangian approach (Monsen *et al.* 2002) where such an approach allows the user to simulate tracers to be released at the initial time throughout the whole region of interest and are tracked until they leave the domain of interest. This approach, however, requires the simulation of a large number of tracers to achieve high resolution for any initial time and any initial location, making the task again quite extensive. A compromise approach can be made by dividing the domain into a small number of subregions Ω_i, $(i = 1, \ldots n)$. The mean residence times are computed for each subregion. This method is adopted in this study.

The reconstructed Qilihai Lagoon is divided into nine different subregions (Figure 2(c)).

To compute the mean residence time for each subregion Ω_i, the concentrations of passive tracers at the boundary conditions are all set to 0. However, the initial concentrations of the passive tracers within the interior of the domain are different and set as follows:

$$C_i(t_0, x \in \Omega_i) = 1 \text{ and } C_i(t_0, x \notin \Omega_i) = 0, \ i = 1, \ldots, n \quad (6)$$

Finally, we can compute the mean residence time of the initial water from subregion Ω_i at time t_0 as:

$$R_i(t_0) = \frac{\int_0^\infty \int_\Omega H(t, x) C_i(t, x) \mathrm{d}x \mathrm{d}t}{\int_{\Omega_i} H(t_0, x) C_i(t_0, x) \mathrm{d}x} \quad (7)$$

in which x represents the horizontal coordinates (x, y). The simulations were all run for a long time to ensure that most of the tracers left the lagoon: less than 0.5% of the initial
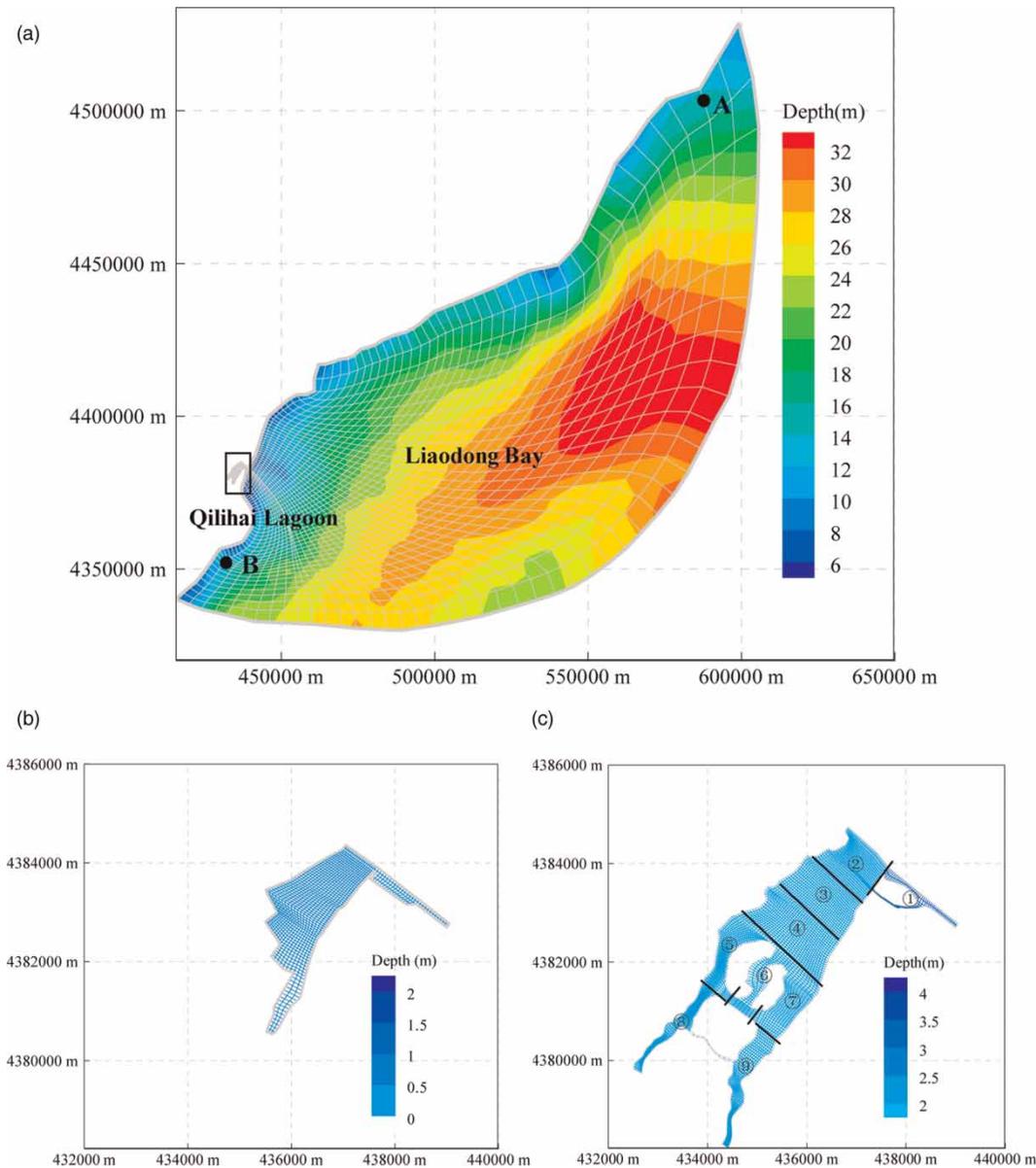

Figure 2 │ Computational domain and structured grid used. (a) Whole computational domain, including the Qilihai Lagoon and part of the sea of the Liaodong Bay. (b) The present configuration grid for the Qilihai Lagoon. (c) The reconstructed configuration grid for the Qilihai Lagoon. The region was divided into nine subregions to compute the water renewal timescales.

tracer was still in the region at the end of the simulation (Brauwere *et al.* 2011).

To calculate the residence time, the hydrodynamic computation is performed for the whole region, including the Qilihai Lagoon and part of Liaodong Bay (Figure 2(a),(c)), while the tracer computation is performed for a spatial region that includes only the Qilihai Lagoon (Figure 2(c)).

Exposure time

The residence time focuses on the time taken for water parcels to leave the domain of interest for the first time. According to this definition, the water parcels must vanish at the boundary of the region of interest, and the water parcels leaving the domain at certain times are not allowed to return. Consequently, this timescale may significantly underestimate the total time spent in the region of interest in tidal systems where water parcels close to the boundary will leave and return to the region several times before escaping completely.

Therefore, exposure time (E) is introduced and is defined as the accumulated time spent by a water parcel in the region of interest before the water parcel leaves the region definitively. The computation of exposure time is very similar to that of residence time, as outlined above. The equation governing the tracer from region i and the initial condition is also similar to Equations (5) and (6). However, the numerical model should simulate the spatio-temporal evolution of tracers in a region larger than the region of interest. Additionally, the computation domain should cover the regions where the whole process occurs so that the water parcels leave the control region on the ebb tide, mix with fresh water in the open sea, and return to the region of interest on the flood tide. For the computation of exposure time in the reconstructed Qilihai Lagoon, the computation domain of tracer transport is the same as the computation domain used for the hydrodynamics (Figure 2(a),(c)).

Brauwere *et al.* (2011) introduced the return coefficient to judge the relative difference between exposure time and residence time

$$r = \frac{E - R}{E} \tag{8}$$

The return coefficient r is between 0 and 1, indicating that no water parcels return after leaving the control domain when the return coefficient is equal to 0. The other limit value ($r = 1$) reveals that the water parcels leave the control region quickly and return after a very long time.

Connectivity

The exposure time is approximately the time taken for water parcels to leave the entire region of interest. Decomposing the exposure time into each subregion results in additional timescales that represent the time that water parcels released from subregion Ω_i spend in each subregion Ω_j, ($j = 1, \ldots . n$), which can be computed as:

$$E_{i,j}(t_0) = \frac{\int_0^\infty \int_{\Omega_j} H(t, x) C_i(t, x) \mathrm{d}x \mathrm{d}t}{\int_{\Omega_i} H(t_0, x) C_i(t_0, x) \mathrm{d}x} \tag{9}$$

in which $E_{i,j}$ represents the time that the water parcel released from subregion Ω_i spent in each subregion Ω_j. For the special case $i = j$, $E_{i,j}$ reveals how long the water parcels released from subregion Ω_i spend in subregion Ω_i.

A dimensionless quantity can then be proposed:

$$d_{i,j} = \frac{E_{i,j}(t_0)}{E_i(t_0)} = \frac{E_{i,j}(t_0)}{\sum\limits_{j=1}^n E_{i,j}(t_0)} \tag{10}$$

in which $d_{i,j}$ expresses the ratio between the time spent in subregion Ω_j and the total time spent in the whole region of interest by the water parcels released from subregion Ω_i. It is obvious that $\sum^n d_{i,j} = 1$, and if the value is close to 1, the time that the water parcels released from subregion Ω_i spend in subregion Ω_j is very long. In other words, the water parcels released from subregion Ω_i spend most of their time in subregion Ω_j. All $d_{i,j}$ values can form an $i \times j$ matrix, which is called a connectivity matrix. The matrix can provide the spatial connection between different subregions and can reveal pollutant diffusion and transport in the lagoon. For example, row i can identify which areas of the domain will be most affected by a pollution source in subregion Ω_i.

MODEL APPLICATION

Framework of the simulations

The case of the Qilihai Lagoon was proposed in this study and two structured grids were used to model it. One grid represented the present configuration of the lagoon (Figure 2(a),(b)) and was applied for model calibration and validation. The other grid represented the configuration of the lagoon after reconstruction (Figure 2(a),(c)) and was used for studying the water renewal capacity in the reconstructed lagoon. The grid used in the calibration and verification (present configuration) contained 2,906 elements, with the smallest element having a length of ~40 m. The reconstructed configuration grid contained 6,238 elements, with the smallest element having a length of ~6 m. Two evenly distributed layers were employed in the vertical direction. The model was numerically integrated with a time step of 2s during the whole simulation period.

The model was driven by surface wind stress and tide. The daily wind data were provided by the China Meteorological Data Sharing Service System (http://cdc.cma.gov.cn/index.jsp). The tide can be synthesised as follows:

$$\zeta = \sum_{i=1}^{n} f_i H_i \cos\left(\sigma_i t + (V_0 + u)_i - g_i\right) \quad n = 9 \tag{11}$$

In which, f_i and u_i are the nodal modulation amplitude and phase corrections, respectively, of tidal constituent i; σ_i is the frequency of tidal constituent i; and V_{0i} is the astronomical argument phase angle. The quantities H_i and g_i are harmonically analysed constants that represent the maximum amplitude and phase lag, respectively.

The initial conditions were set for water level and flow velocity. The initial water level was set as the average value of the initial water level on the sea boundary. The initial flow velocity was set as 0 m s^{-1}.

Model calibration and validation

The Qilihai Lagoon model was calibrated using field data measured at Station A. (Figure 2(a), 120°57′38.91″ E 40°41′46.23 N, measured from 10 August to 11 August 2006) (Li 2008). The root mean squared error (RMSE)

(Chau *et al.* 2005; Lin *et al.* 2006; Wang *et al.* 2012), common statistical measures R^2, average error (AE) and average absolute deviation δ (Azamathulla *et al.* 2010; Nazafzadeh & Azamathulla in press) were used for calibration and validation. The RMSE values should be compared with the local tidal amplitude. If these values are lower than 5% of the local amplitude, the agreement between model results and observations should be considered excellent; if they range between 5 and 10% of the local amplitude, the agreement should be considered very good (Dias *et al.* 2009).

In the EFDC Model, the vertical turbulent viscosity A_v and the vertical turbulent diffusivity A_b can be calculated based on the Mellor–Yamada (M–Y) turbulence closure scheme (Mellor & Yamada 1982). Parameters related to the Mellor and Yamada turbulence model are set to the same values as those used in other hydrodynamic models, such as the Princeton Ocean Model and the Estuary, Coastal and Ocean Model (HydroQual Inc. 2002). The horizontal diffusion coefficient A_H is determined by Smagorinsky (Smagorinsky 1963), and the non-dimensionless viscosity parameter in the Smagorinsky formula is set to a constant value of 0.2 (Berntsen 2002).

Bottom roughness (n in the Manning equation $C = \frac{1}{n} R^{1/6}$) was changed from 0.025 to 0.032 until a reasonable agreement was reached between the model and the
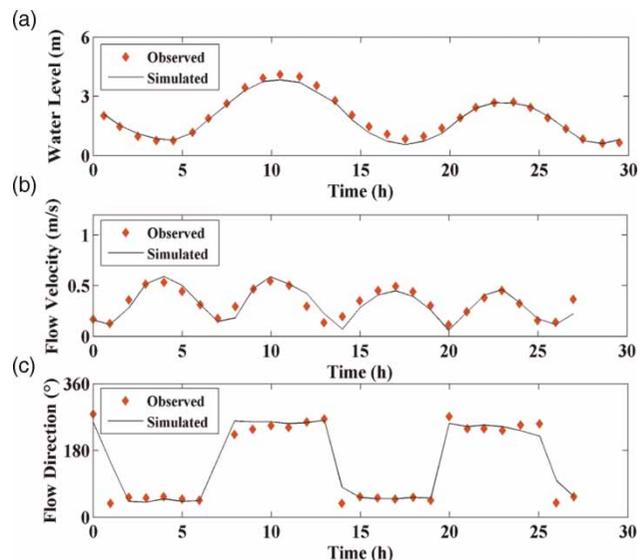

Figure 3 | Time series of simulated data (solid lines) and observed data (circle dots) at Station A.

observations. Figure 3 shows comparisons of model-simulated water levels, flow velocity and flow direction against observed data for Station A. Table 1 shows the R^2, RMSE, AE and δ for water level, flow velocity and flow direction.

The other set of observed data measured at Station B (Figure 2(a), 119°01'03.99″ E, 39°11'44.82 N, measured from 28 September to 29 September 2000) (Hu 2007) was used to verify the model performance. Figure 4 shows comparisons of model-simulated water levels, flow velocity and flow direction against the observed data for Station B. The R^2, RMSE, AE and δ for water level, flow velocity and flow direction can also be observed in Table 1. The agreement between the simulated and observed values was very good in water levels. Although the errors were not negligible for flow velocity and flow direction, and some temporal shifting was observed for them, they were still

acceptable. Firstly, there might be some errors due to the terrain model used for numerical simulation. Secondly, the bottom roughness in the simulation was set to a constant value and not varying in the domain according to the real situation. The results show that the model could adequately simulate hydrodynamic conditions in the lagoon.

The calibrated model was used to study the water renewal capacity in the reconstructed lagoon. Several simulations were performed to reproduce the effect induced by tide, the depth of the inlet and wind. Three series of simulations were investigated. In the first scenario, only the tide was considered to force the basin and the depth of the inlet was set to 3.5 m. In the second scenario, two typical winds (southwest and northeast) with a constant magnitude of 5 m s^{-1} are prescribed together with the tide, with the same depth as in scenario one. In the third scenario, only the tide forces the basin, and the depth of the inlet increases from 2.5 to 6.0 m in increments of 0.5 m.

Table 1 | The R^2, RMSE, AE and δ for water level, flow velocity and flow direction

Parameter	Location	R^2	RMSE (%)	AE	δ
Water levels (m)	Station A	0.98	4.25	4.87	6.87
	Station B	0.95	4.47	−2.94	5.11
Flow velocity (m/s)	Station A	0.86	11.27	5.62	13.83
	Station B	0.77	13.42	−8.47	16.34
Flow direction (°)	Station A	0.92	10.37	−9.46	11.62
	Station B	0.62	18.40	14.63	18.29

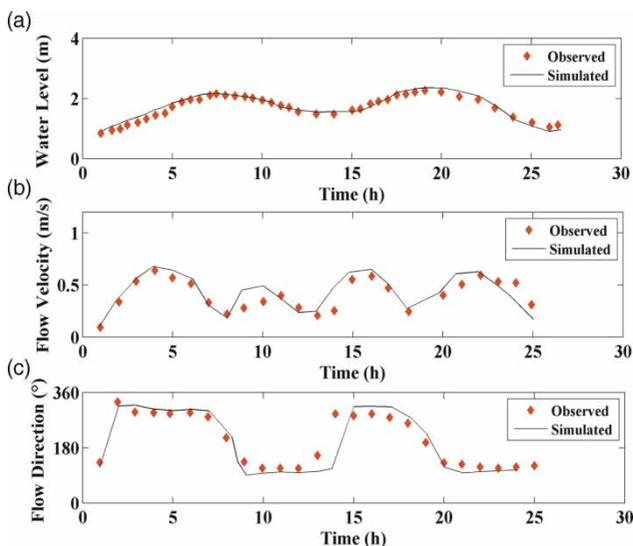## RESULTS OF SIMULATIONS AND DISCUSSION

Characteristics of water renewal

Figure 5 shows the residence and exposure times for the nine subregions in scenario one. The residence times for the areas that were close to the inlets were less than 20 days, mainly because these areas can be directly influenced by the sea. The residence times abruptly became longer in the inner lagoon areas, at approximately 306, 208 and 206 days for subregions 5, 6 and 7, respectively. The values all exceeded 700 days in the end lagoon areas (subregions 8 and 9). The long residence times in these areas could be explained by two factors. One is that the tide inlet connecting the lagoon and the sea was so narrow that the waters in the inner and end lagoon areas could not be directly exchanged with sea water during a flood cycle. The other factor was the shape of the lagoons. The water in the inner lagoon areas was divided into several parts by artificial islands, and the water transport and diffusion were hindered by these artificial islands. Thus, the residence times in these regions abruptly became longer and increased toward the end of the lagoon.
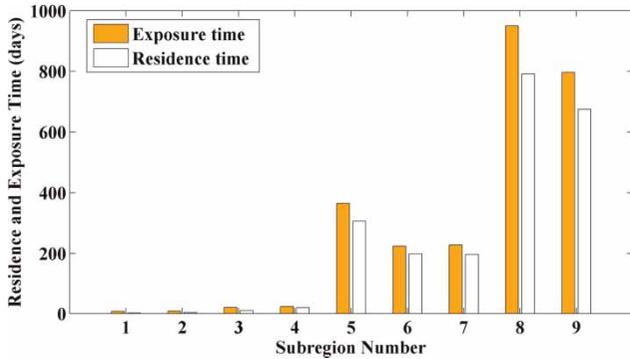

Figure 4 | Time series of simulated data (solid lines) and observed data (dotted lines) at Station B.

998   X. Gao et al.   Water renewal timescales in a lagoon in China

Journal of Hydroinformatics | 15.3 | 2013

Figure 5 | Comparison between residence time and exposure time when only tide forces the circulation.

The distribution of exposure time was very similar to that of residence time. However, the exposure times were always larger than residence times, allowing water parcels to leave and return to the region of interest several times. The return coefficients for the nine subregions are shown
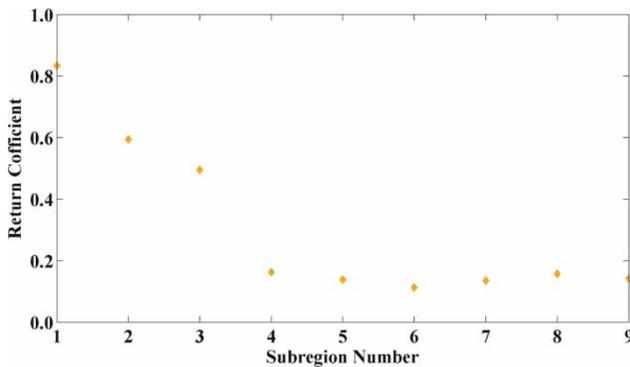

Figure 6 | Return coefficients for subregions 1–9 when only tide forces the circulation.

in Figure 6. It is obvious that the return coefficients increased toward the open boundary of the domain. The highest return coefficient was in subregion 1 (approximately 0.9) indicating that almost all the tracers for subregion 1 have been ejected to open sea and returned to the lagoon during the next flood event. In the inner and end lagoon areas, the return coefficients were all lower than 0.2, suggesting that the return waters have a slight influence on these areas.

The connectivity matrix is a useful tool for describing the pollutant transport and diffusion from a pollution source. The connectivity matrix under the no wind condition in Qilihai Lagoon is shown in Figure 7(a). One can see that the water from the pollution source did not spend the same amount of time in each subregion, and it spent relatively more time in some subregions than others during its journey out of the lagoon. For example, the water parcels from subregion 3 spent more time in subregions 2–5. The water parcels spent most of their time in their original subregion and the subregions nearby, which indicates that the pollutants under the no wind condition were not removed easily and that the areas near the pollution source were mostly affected by pollution. The water parcels from subregions 5–7 tended to spend relatively more time in subregion 4 and relatively less time in subregions 1–3. The former result could be due to the volume of subregion 4, which is nearly 1.8 times the volume of subregion 5, 2.3 times the volume of subregion 6 and 1.5 times the volume of subregion 7. The less time spent in subregions 1–3 indicates that the return water may not play an important role in the water in these areas.
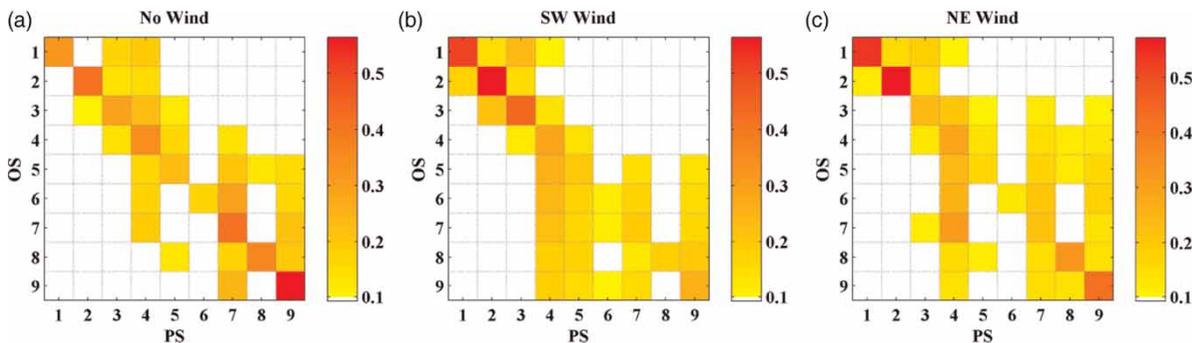

Figure 7 | Connectivity matrices under (a) no wind, (b) southwest wind, and (c) northeast wind. OS stands for 'originating subregion', where the water parcels were released at the initial time; PS stands for 'passing subregion', where the water parcels released from the originating subregion pass during their journey out of the region.

Influence of wind on water renewal

In scenario two, only exposure time and connectivity were used as a water renewal timescale because exposure time is more informative than residence time for a tide system. The exposure times for the nine subregions under the three conditions (no wind, southwest wind and northeast wind) are shown in Figure 8. The results suggest that the winds could enhance water exchange significantly in the inner and in the end lagoon areas (subregions 5–9). In subregion 8, for example, when the wind directions were northeast and southwest, the exposure times were 186 and 346 days, respectively, 764 and 604 days less than the exposure times under the no wind condition. The best wind direction for water exchange in the Qilihai Lagoon was northeast. The exposure times in the Qilihai Lagoon were all less than 200 days in this situation. The action of this type of wind enhanced the lagoon's environmental physical cleaning capacity. This wind is dominant in autumn, so this appears to be the best time for diluting pollutants in the lagoon.

The results under the wind conditions showed greater connectivity, possibly because the winds enhanced the mixture between the waters in the lagoon (Figure 7(b),(c)). With the southwest wind forcing, the pollutants released from the end lagoon areas tended to spend more time in the inner lagoon areas. For example, the pollutant from subregion 9 spent most of its time in subregion 7 under the no wind condition (Figure 7(a)) and in subregions 4–7 under the southwest wind condition (Figure 7(b)). With northeast wind forcing, the pollutants released from the head lagoon areas tended to spend more time in the inner and end lagoon areas. For example, the pollutant from subregion 3 spent most of its time in subregions 2–5 under the no wind condition (Figure 7(a)) and in subregions 3–5, 7 and 9 under the northeast wind condition (Figure 7(c)). Similarly, under the no wind condition, the water parcels from subregions 5–9 all spent relatively more time in subregion 4 during their journey out of the lagoon. The results indicate that subregion 4 was the most easily affected and should always be focused on no matter which subregion was polluted in the lagoon.

Influence of inlet depth on water renewal

The exposure times for the nine subregions under different inlet depths are shown in Figure 9. The results suggest that the inlet depth had a great influence on the water renewal capacity in the lagoon. As expected, the increase in inlet depth resulted in a better water exchange. However, the increase rate of water exchanges in the various cases was different. The results show that the maximum change was obtained with an inlet depth of 4.0 m, the increasing rate of water exchanges for subregions 1–9 were all higher than 40% when the inlet depth increased from 2.5 to 4.0 m. There were no significant increases in water exchanges when the depth increased from 4.0 to 6.0 m. Thus, it can be concluded that the optimal inlet depth to improve the water exchange in the whole lagoon is approximately 4.0 m.

Figure 10 shows the connectivity matrix under different inlet depths from 2.5 to 6.0 m. The connectivity matrices
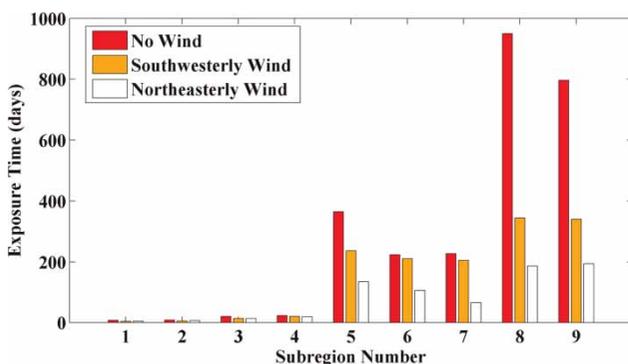

Figure 8 │ Exposure times for subregions 1–9 under three conditions (no wind, southwest wind and northeast wind).
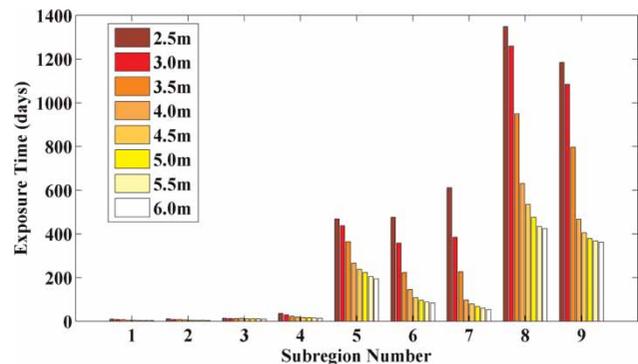

Figure 9 │ Exposure time for subregions 1–9 under different inlet depths, from 2.5 to 6.0 m, in increments of 0.5 m.

were similar under the different depths. The water parcels always tended to spend most of their time in the areas around their original subregion in all cases. Subregion 4 should always be focused on because it is so easily polluted no matter where the pollution source is and what the depth of the inlet is. The results show that the inlet depth did not change the distribution of pollutants during their journey out of the lagoon.

CONCLUSIONS

The aim of this paper is to provide information for the ecological restoration planning of the Qilihai Lagoon using the concept of residence time, exposure time and connectivity. The main conclusions of the study are as follows.

The lagoon under the no wind condition exhibited a low water renewal capacity, and the exposure times in the end areas all exceeded 700 days. Thus, the water quality in these areas should be given attention by managers. The connectivity matrix showed that the pollutants from pollution source did not spend the same amount of time in each subregion before leaving the region of interest definitively, and the areas most affected by pollution were those around the pollution source in the no wind condition. This information may be useful for managers when identifying areas that need to be protected when pollution events occur.

Wind action could improve the water renewal capacity in the lagoon significantly, and the exposure times in the

wind condition were all lower than 400 days in the whole region, especially for northeast wind, the exposure times were all below 200 days. Thus, autumn, with its dominant northeast winds, appeared to be the best time for removing pollutants in the lagoon. The connectivity in the lagoon was also changed by the wind action. The areas that were most affected were not limited to the areas around the pollution source. The inner and end lagoon areas should also be considered under southwest and northeast winds, respectively.

Increasing the inlet depth would not necessarily provide a better exchange. The results showed that the lagoon improved its water renewal capacity by 40% when the inlet depth increased from 2.5 to 4.0 m. However, there were no significant increases in water renewal capacity when the depth increased from 4.0 to 6.0 m. Thus, the optimal inlet depth for water renewal in the lagoon is approximately 4.0 m. The connectivity matrices under the different inlet depths were similar, indicating that the increases in inlet depth could shorten the time taken by pollutant removal, but could not change the distribution of pollutants during their journey out of the lagoon.

In this study, we paid more attention to the physical processes of these pollutants, such as transport and diffusion, while neglecting ecological processes. The next step will be to investigate the fate of dissolved pollutants under integrated physical and ecological processes, and we hope these works will be useful for scientists and managers studying the Qilihai Lagoon.
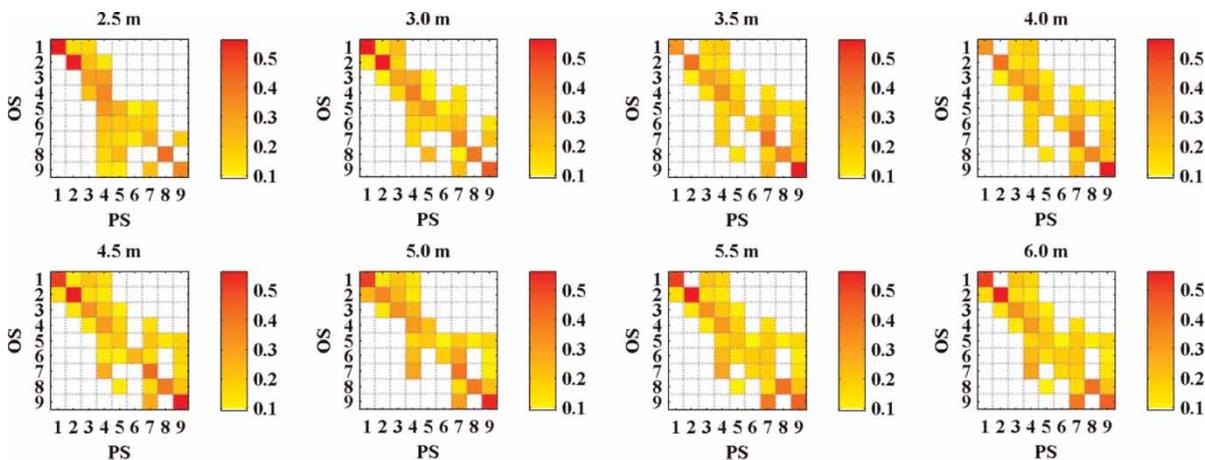

Figure 10 │ Connectivity matrices under inlet depths of 2.5–6.0 m in increments of 0.5 m.

REFERENCES

Arega, F., Armstrong, S. & Badr, A. W. 2008 Modeling of residence time in the East Scott Creek Estuary, South Carolina, USA. *Journal of Hydro-environment Research* **2**, 99–108.

Azamathulla, H. M., Ghani, A. A., Zakaria, N. A. & Guven, A. 2010 Genetic programming to predict bridge pier scour. *Journal of Hydraulic Engineering ASCE* **136**, 165–169.

Berntsen, J. 2002 Internal pressure errors in sigma-coordinate ocean models. *Journal of Atmospheric and Oceanic Technology* **19** (9), 1403–1414.

Brauwere, A. D., Brye, B. D., Blaise, S. & Deleersnijder, E. 2011 Residence time, exposure time and connectivity in the Scheldt Estuary. *Journal of Marine Systems* **84**, 85–95.

Brye, B. D., Brauwere, A. D., Gourgue, O., Delhez, E. J. M. & Deleersnijder, E. 2012 Water renewal timescales in the Scheldt Estuary. *Journal of Marine Systems* **94**, 74–86.

Chau, K. W., Wu, C. L. & Li, Y. S. 2005 Comparison of several flood forecasting models in Yangtze River. *Journal of Hydrologic Engineering ASCE* **10**, 485–491.

Cucco, A. & Umgiesser, G. 2006 Modeling the Venice Lagoon residence time. *Ecological Modelling* **193**, 34–51.

Delhez, E. J. M. 2006 Transient residence and exposure times. *Ocean Science* **2**, 1–9.

Delhez, E. J. M. & Deleersnijder, E. 2006 The boundary layer of the residence time field. *Ocean Dynamics* **56**, 139–150.

Delhez, E. J. M., Heemink, A. W. & Deleersnijder, E. 2004 Residence time in a semi-enclosed domain from the solution of an adjoint problem. *Estuarine Coastal and Shelf Science* **61**, 691–702.

Dias, J. M., Sousa, M. C., Bertin, X., Fortunato, A. B. & Oliveira, A. 2009 Numerical modeling of the impact of the Ancao Inlet relocation (Ria Formosa, Portugal). *Environmental Modelling & Software* **24**, 711–725.

Hamrick, J. M. 1992 *A Three-Dimensional Environmental Fluid Dynamics Computer Code: Theoretical and Computational Aspects*. Special Report No. 317 in Applied Marine Science and Ocean Engineering. College of William and Mary, Virginia Institute of Marine Science, USA, 63 pp.

Hu, X. M. 2007 *Water Quality Numerical Simulation and Eutrophication Assessment in the Liaodong Bay*. Dalian University of Technology, China, 37 pp.

HydroQual Inc. 2002 *A Primer for ECOMSED, Version 1.3, User's Manual*. HydroQual Inc., 1 Lethbridge Plaza, Mahwah, NJ, 188 pp.

Ji, Z. G., Hamrick, J. M. & Pagenkopf, J. 2002 Sediment and metals modeling in shallow river. *Journal of Environmental Engineering* **128**, 105–119.

Jin, K. R. & Ji, Z. G. 2004 Case study: modeling of sediment transport and wind-wave impact in Lake Okeechobee. *Journal of Hydraulic Engineering, ASCE* **130**, 1055–1067.

Li, W. D. 2008 Numerical modeling of tidal current and sediment in Huludao sea area. *Journal of Waterway and Harbor* **29**, 94–99.

Li, Y. P., Acharya, K. & Yu, Z. B. 2011 Modeling impacts of Yangtze River water transfer on water ages in Lake Taihu, China. *Ecological Engineering* **37**, 325–334.

Lin, J. Y., Cheng, C. T. & Chau, K. W. 2006 Using support vector machines for long-term discharge prediction. *Hydrological Sciences Journal* **51**, 599–612.

Mellor, G. L. & Yamada, T. 1982 Development of a turbulence closure model for geophysical fluid problems. *Reviews of Geophysics* **20**, 851–875.

Monsen, N. E., Cloern, J. E., Lucas, I. Y. & Monismith, S. G. 2002 A comment on the use of flushing time, residence time, and age as transport time scales. *Limnology and Oceanography* **47**, 1545–1553.

Nazafzadeh, M. & Azamathulla, H. M. Group method of data handling to predict scour depth around bridge piers. *Neural Computing & Applications*, in press, doi: 10.1007/s00521-012-1160-6.

Ribbe, J., Wolff, J., Staneva, J. & Grawe, J. 2008 Assessing water renewal time scales for marine environments from three-dimensional modeling: a case study for Hervey Bay, Australia. *Environmental Modeling & Software* **23**, 1217–1228.

Sebnem, E. 2008 Effects of thermal stratification and mixing on reservoir water quality. *Limnology* **9**, 135–142.

Shen, Y. M., Wang, J. M., Zheng, B. H., Feng, Y., Wang, Z. X. & Yang, X. 2011 Modeling study of residence and water age in Dahuofang Reservoir in China. *Science China-Physics Mechanics & Astronomy* **54**, 127–142.

Smagorinsky, J. 1963 General circulation experiments with the primitive equations: I. The basic experiment. *Monthly Weather Review* **91**, 99–164.

Wang, W. C., Cheng, C. T., Chau, K. W. & Xu, D. M. 2012 Calibration of Xinanjiang model parameters using hybrid genetic algorithm based fuzzy optimal model. *Journal of Hydroinformatics* **14**, 784–799.

Zhang, C., Gao, X. P., Wang, L. Y. & Chen, Y. Y. Analysis of agricultural pollution by flood flow impact on water quality in a reservoir using a three-dimensional water quality modeling. *Journal of Hydroinformatics*, in press, doi: 10.2166/hydro.2012.131.